RESEARCH PAPER

Preparation of CuO nanoparticles by metal salt-base reaction in aqueous solution and their metallic bonding property

**Y. Kobayashi · T. Maeda · K. Watanabe ·
K. Ihara · Y. Yasuda · T. Morita**

Abstract This article describes a method for preparing CuO nanoparticles in aqueous solution, and a demonstration of feasibility of metallic bonding with the use of the CuO particles. Colloid solution of CuO nanoparticles was prepared from $Cu(NO_3)_2$ aqueous solution (0.01 M) and NaOH aqueous solution (0.019 M) at 5–80 °C. Leaf-like aggregates with an average size of 567 nm composed of CuO nanoparticles were produced at 20 °C. The size of leaf-like aggregates decreased with increasing reaction temperature. Metallic copper discs could be bonded using the CuO nanoparticles under annealing at 400 °C and pressurizing at 1.2 MPa for 5 min in H_2 gas. A shear strength required for separating the bonded discs was 25.4 MPa for the CuO nanoparticles prepared at 20 °C, whose aggregates were the largest among the CuO particles examined. These results indicated that the formation of leaf-like aggregates of CuO nanoparticles led to efficient metallic bonding.

Introduction

A bonding technique is quite required to connect solid state materials in various fields such as civil engineering, construction industry, and electronics (Matsuoka and Imai 2009). In bonding of metallic materials, a process of annealing and pressurizing is usually used (Weisman 1976). This process provides diffusion of their components on their interface, and consequently the metallic materials are bonded. To avoid damage of the metallic materials that are exposed to high temperature during bonding, temperature for bonding is desired to be lowered.

A new bonding technique utilizing metallic nanoparticles has been reported (Morita et al. 2008a; Ide et al. 2005; Akada et al. 2008; Murray et al. 2006; Moon et al. 2005). As the size of metallic particles reaches several nanometers, their melting point decreases (Takagi 1954; Buffat and Borel 1976). Accordingly, the bonding can be helped by inserting the metallic nanoparticles between the metallic materials. Among metallic powders, copper particles are promising materials for the metallic bonding, because of low cost. However, they face at a problem of easy oxidation in air (Kanninen et al. 2008; Park et al. 2007), which spoils bonding properties.

Y. Kobayashi (✉) · T. Maeda · K. Watanabe · K. Ihara
Department of Biomolecular Functional Engineering,
College of Engineering, Ibaraki University,
4-12-1 Naka-narusawa-cho, Hitachi, Ibaraki 316-8511,
Japan
e-mail: ykoba@mx.ibaraki.ac.jp

Y. Yasuda · T. Morita
Hitachi Research Laboratory, Hitachi Ltd., 7-1-1
Omika-cho, Hitachi, Ibaraki 319-1292, Japan

Copper in oxidative state, such as copper oxide, is available as a precursor of metallic copper, since it can be reduced to metallic copper with reducing agent or reducing atmosphere. Therefore, the copper oxide may be also available as insertion powders for bonding metallic materials. Copper oxide nanoparticles are expected to be transformed to metallic copper nanoparticles during bonding in reducing atmosphere. Simultaneously, the metallic copper nanoparticles will bond the metallic materials.

CuO nanoparticle aqueous colloid solution can be easily prepared in aqueous solution. Lee et al. (1997) reported preparation of uniform colloidal copper oxide by a controlled double-jet technique using $Cu(NO_3)_2$ aqueous solution and NaOH aqueous solution, and studied on its formation mechanism. Liu et al. (2006) prepared CuO particles by a hydrothermal process using cupric dodecylsulfate aqueous solution and NaOH aqueous solution. The obtained particles were single-crystalline, and their structure was platelet. Zheng and Liu synthesized CuO hierarchical nanosheets at mild conditions (near-neutral pH and near-room temperature) using $Cu(CH_3COO)_2$ aqueous solution and ammonia solution, and growth mechanism of the CuO nanosheets was also studied (Zheng and Liu 2007).

The aim of this work is to examine CuO nanoparticles as the insertion powder for metallic bonding. Aqueous colloid solution of the CuO nanoparticles was prepared by mixing $Cu(NO_3)_2$ and NaOH in water A relation of their metallic bonding properties to morphology of the particles was studied on.

Experimental

Chemicals

Copper (II) nitrate trihydrate $(Cu(NO_3)_2 \cdot 3H_2O)$ (Kanto Chemical Co., Inc., 77.0–80.0% (as $Cu(NO_3)_2$)) and sodium hydroxide solution (NaOH) (Kanto Chemical Co., Inc., 1 M) were used as CuO precursors. All chemicals were used as received. Water that was ion-exchanged and distilled with Yamato WG-250 was used in all the preparations.

Preparation

Colloid solutions of CuO nanoparticles were synthesized by metal salt-base reaction. An aqueous solution of NaOH (1 M) (19 mL) was added to 981 mL of 0.0102 M $Cu(NO_3)_2$ aqueous solution under vigorous stirring at 5–80 °C, which resulted in a Cu^{2+} concentration of 0.01 M in the final solution. The reaction times were 14 days, 1 day and 12 h for the reaction temperatures of 5, 20–30, and 50–80 °C, respectively.

Characterization

The CuO particles were characterized by transmission electron microscopy (TEM), electrophretic light scattering (ELS), X-ray diffractometry (XRD) and thermal analysis (TG-DTA). TEM photographs were taken with a JEOL JEM-2000FX II microscope operating at 200 kV. Samples for TEM were prepared by dropping and evaporating the particle colloid on a collodion-coated copper grid. Dozens of particle diameters in TEM images were measured to determine number-averaged particle size and standard deviation of particle size distribution. To measure ζ-potential of particles, ELS was performed with a Brookhaven ZetaPALS instrument. HCl aqueous solution or NaOH aqueous solution was added to solution to vary pH of solution for the ELS measurement. XRD measurements were carried out with a Rigaku RAD-B X-ray diffractometer at 50 kV and 150 mA with $CuK\alpha_1$ radiation. For preparing a powder sample for the XRD measurement, supernatant of the particle colloid was removed with decantation, and then residue of the colloid was dried at room temperature for 24 h in vacuum. TG-DTA was performed in 3% (v/v) H_2/N_2 gas at a heating rate of 10 °C/min with a Mettler-Toledo TGA/SDTA851 thermal analyzer. Samples for TG-DTA were obtained in the same manner as that for the XRD samples.

Metallic bonding property was investigated by the same set-up as used in our previous works (Morita et al. 2008a, b, 2009; Yasuda et al. 2009). Powder samples were sandwiched between copper and aluminum discs (a stage (diameter: 10 mm, thickness: 5 mm) and a plate (diameter: 5 mm, thickness: 2.5 mm)), and pressed at 1.2 MPa under annealing in H_2 at 400 °C for 5 min with a Shinko Seiki vacuum reflow system. Then, shear stress, which was required to separate the bonded stage and plate, was measured with a Seishin SS-100KP bond tester. The discs were observed with a JEOL JSM-5600LV microscope after the measurements of shear strengths.

Results and discussion

Morphology of particles

Figure 1 shows photographs of colloid solutions prepared at various reaction temperatures. At a reaction temperature of 5 °C, a blue, clear $Cu(NO_3)_2$ solution turned a blue, opaque colloid solution, which indicated that $Cu(OH)_2$ particles were produced. For reaction temperatures of 20–80 °C, a $Cu(NO_3)_2$ aqueous solution turned brown after the turn to the blue, opaque colloid solution, which implied production of CuO particles. Figure 2 shows TEM images of as-prepared particles. At 5 °C, submicron-sized aggregates irregular in size and shape were produced. For 20 °C, leaf-like aggregates with a longitudinal size of ca., 600 nm and a lateral size of ca., 400 nm were produced. A high magnification image (inset of the Fig. 2) revealed that the aggregates were composed of nanoparticles with a size of ca., 10 nm, which was roughly estimated with TEM observation since outlines of the nanoparticles were not clear-cut. A value of pH was 4.8 prior to addition of NaOH. The pH reached a peak of 6.8 at 3 h after the addition, and then gradually decreased. Finally, it leveled out at 6.2 in 24 h. A plot (a) in Fig. 3 shows ζ-potential of the CuO nanoparticles prepared at 20 °C as a function of pH. The CuO nanoparticles had an iso-electric point (i.e.p.) of ca., 10.2. Accordingly, the pH approached from the initial pH of 4.8 to the i.e.p. with no going above the i.e.p. with the addition of NaOH. During the approach, the Cu nanoparticles formed the aggregates.

The aggregates appeared to become small with an increase in reaction temperature. In Fig. 4, an average size of the aggregates is plotted versus the reaction temperature. The average sizes of the aggregates were estimated as a number-average of the longitudinal size and the lateral size. The aggregate size increased from 567.1 ± 52.0 to 39.5 ± 13.7 nm with an increase in the reaction temperature from 20 to 80 °C. In the case of 80 °C, a value of pH reached a maximum rapidly compared with other temperatures, then decreased, and finally leveled out at 5.9 in 12 h. This pH was lower than the pH of 6.2 for 20 °C. A plot (b) in Fig. 3 shows ζ-potential of the CuO nanoparticles prepared at 80 °C as a function of pH. The CuO nanoparticles had an i.e.p. of ca., 10.9. This i.e.p. was higher than that for 20 °C, though a reason for the high i.e.p. is still unclear. It is worth noting that a difference between the i.e.p. and the final pH was 4.0, which was large compared to the case of 20 °C that was 3.0. This meant that the pH moved away from the i.e.p, and electrostatic repulsion between the particles became active. Consequently, aggregation of particles was controlled at the high temperatures.

The size of nanoparticles that composed the aggregates tended to increase, as the reaction temperature increased. High reaction temperature should accelerate movement of CuO primary particles, i.e., CuO nuclei, which were generated in the solution at initial reaction stage. This acceleration of movement probably increased collision frequency of the nuclei in the solution. Consequently, the nuclei formed CuO particles, and the particles grew intensively, at the high reaction temperatures.
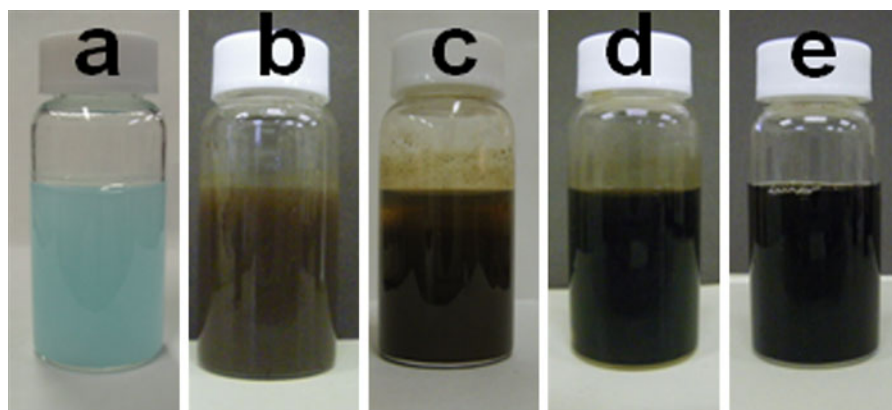

Fig. 1 Photographs of colloid solutions prepared at reaction temperatures of **a** 5, **b** 20, **c** 30, **d** 50, and **e** 80 °C
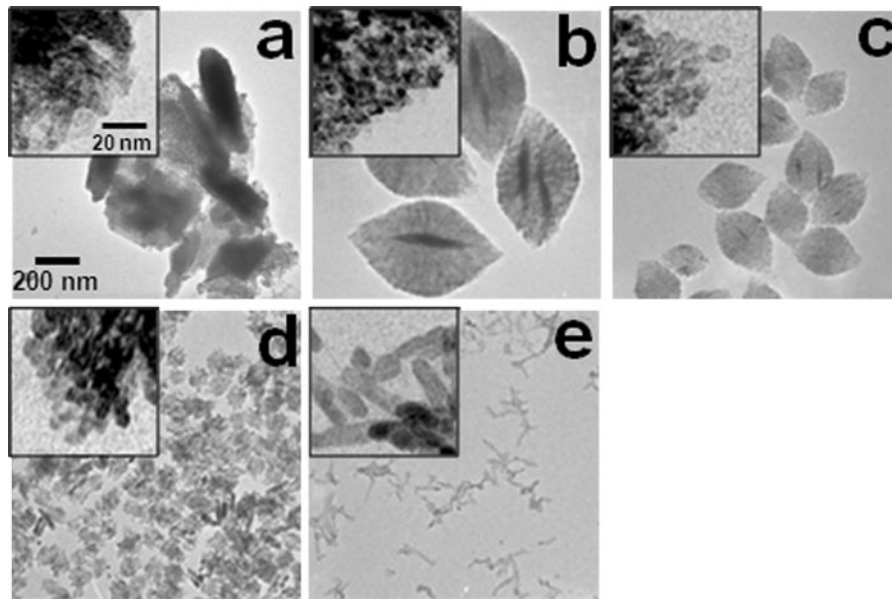
Fig. 2 TEM images of particles prepared at reaction temperatures of **a** 5, **b** 20, **c** 30, **d** 50, and **e** 80 °C
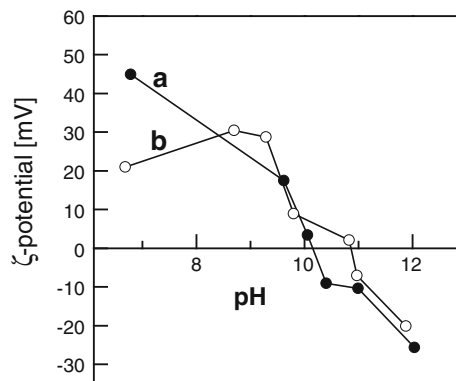

Fig. 3 ζ-potentials of particles prepared at (*a*) 20 and (*b*) 80 °C versus pH

Fig. 4 Plot of the average aggregate size versus the reaction temperature

Figure 5 shows XRD pattern of the as-prepared particles. At a reaction temperature of 5 °C, the pattern was featureless, which indicated that the reaction temperature of 5 °C was too low to drive formation of crystalline copper compounds particles. For 20 °C, several peaks were recorded mainly at 35.6°, 38.8°, and 48.9°. They were attributed to monoclinic CuO (JCPDS card No. 5-0661). Besides the CuO peaks, peaks assigned to $Cu_2(OH)_3NO_3$ (JCPDS card No. 15-0014) were also detected at 12.8° and 25.8°. Over 20 °C, the $Cu_2(OH)_3NO_3$ peaks disappeared, and only the peaks due to CuO were detected. The reaction for formation from $Cu(NO_3)_2$ to CuO was not completed
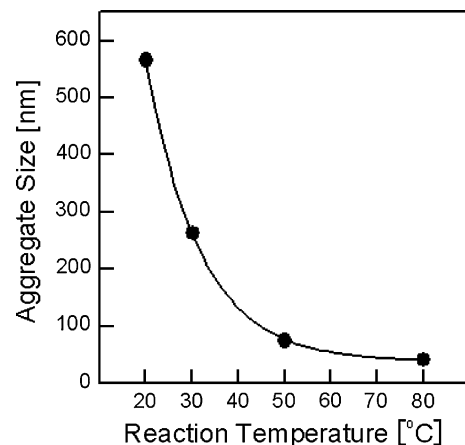
at the temperature as low as 20 °C. Average crystal sizes were estimated from the XRD line broadening of the 35.6° peak according to the Scherrer equation. The sizes were ca., 10 nm; 9.7, 9.6, 11.4, and 9.6 nm for 20, 30, 50, and 80 °C, respectively. There was no large difference among the reaction temperatures examined.

Bonding property

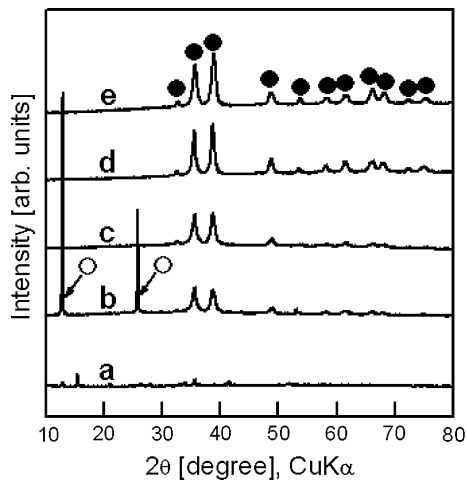TG-DTA curves for the particles prepared at 20 °C are shown in Fig. 6. An endothermic peak and a weight

Fig. 5 XRD patterns of particles prepared at reaction temperatures of (*a*) 5, (*b*) 20, (*c*) 30, (*d*) 50, and (*e*) 80 °C. Symbols (*filled circle*) and (*open circle*) stand for CuO and Cu$_2$(OH)$_3$NO$_3$, respectively

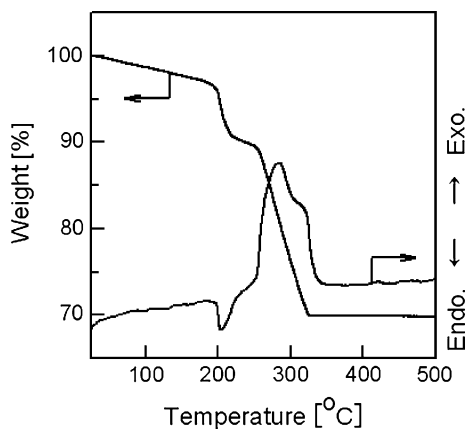**Fig. 7** XRD pattern of aluminum stage after bonding with the use of Cu nanoparticles. The particles were prepared at 20 °C

Fig. 6 TG-DTA curves in 3% (v/v) H$_2$/N$_2$ gas for particles prepared at 20 °C

loss were detected at ca., 200 °C. According to the XRD measurement shown in Fig. 5, the as-prepared metallic Cu particles contained the Cu$_2$(OH)$_3$NO$_3$. According to Lee et al.'s work (Lee et al. 1997), Cu$_2$(OH)$_3$NO$_3$ begins to decompose into CuO at ca., 225 °C under an increase in temperature, which results in a weight loss due to elimination of water and NO$_3$ group. Thus, the weight loss accompanying the endothermic peak detected in the present work was assigned to the decomposition of Cu$_2$(OH)$_3$NO$_3$ into CuO. This result suggested that the annealing made it possible to produce pure CuO even if Cu$_2$(OH)$_3$NO$_3$ was contained as impurity in CuO particles. An

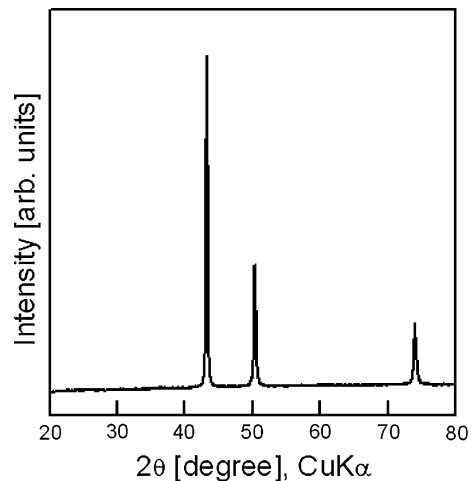exothermic peak and a weight loss were detected in a range of 250–320 °C, and the weight did not change above 320 °C. The weight loss in a range of 250–320 °C was 21.8%, with the respect to the weight at 250 °C. Assuming that all the particles for 250 °C were CuO, the weight loss due to removal of oxygen from the CuO was estimated as 20.8%, which almost corresponded to the measured weight loss of 21.8%. Accordingly, the CuO was completely reduced in the reducing gas to form metallic Cu in the temperature range.

Figure 7 shows XRD pattern of the particles on the aluminum stage after bonding with the use of CuO nanoparticles. The aluminum discs and not the copper discs were used in this XRD measurement for distinguishing peaks of the particles from those of the aluminum stage. The particles were treated with the same manner as the bonding, besides the use of the aluminum discs. Peaks at 43.3°, 50.4°, and 74.1° were attributed to metallic Cu (JCPDS card No. 4-0836), and any other peaks were not detected. This result confirmed that the Cu oxide was completely reduced to metallic Cu, which supported the result given by thermal analysis. Thus, a bonding temperature was adjusted to 400 °C for completing the decomposition of Cu$_2$(OH)$_3$NO$_3$ into CuO and the reduction of CuO to metallic Cu.

Figure 8 shows photographs of the copper stage after the measurement of shear strength. Reddish brown products that were obviously metallic Cu were observed in widespread area on the stage for all the
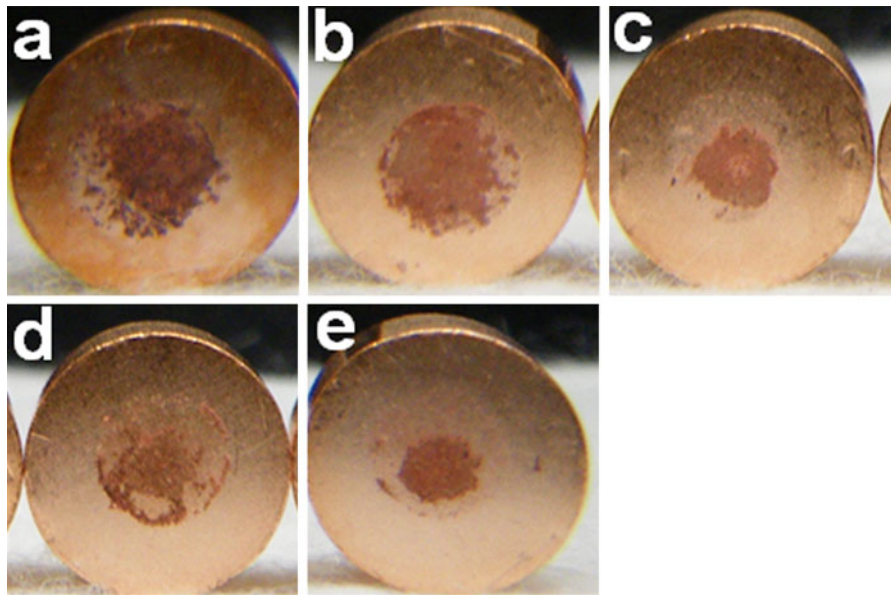
Fig. 8 Photographs of the copper stages after the measurement of shear strength. The particles used for the measurements were prepared at the reaction temperatures of **a** 5, **b** 20, **c** 30, **d** 50, and **e** 80 °C

samples examined. This observation indicated that the as-prepared particles were reduced to metallic Cu annealing in H_2 gas, which was supported with the thermal analysis (Fig. 6) and the XRD measurement (Fig. 7). Consequently, the metallic Cu bonded the copper discs. Though the reddish brown product was also produced for the reaction temperature of 5 °C, the copper discs were not bonded strongly. In contrast, strong bonding was obtained using the CuO particles prepared over 5 °C. Figure 9 shows shear strength as a function of the reaction temperature. A shear strength achieved a value as high as 25.4 MPa for the sample of 20 °C. The data was roughly summarized with a fitting line of an exponential function. The shear strength roughly tended to decrease with the increase in reaction temperature. Figure 10 shows SEM images of surface of the copper plate separated with the shear stress. Particles with a size of ca., 200 nm appeared to be sintered for the reaction temperature of 5 °C. In contrast, for 20 °C, many dimples were observed accompanying with sharp tips on the surface. The dimples tended to disappear with the increase in the reaction temperature. Dimples are formed in bonded region when metals that are strongly bonded are separated with shear stress. Accordingly, this observation supported that the coppers could be strongly bonded using the CuO particles prepared at 20 °C.
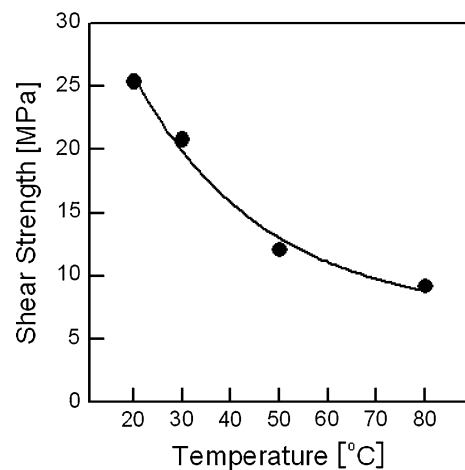

Fig. 9 Plot of the shear strength versus the reaction temperature

According to the TEM observation in the Fig. 2, the leaf-like aggregates produced at 20 °C had the largest aggregate size among the CuO nanoparticles examined. This observation implied that there was a strong dependence of the shear strength on the aggregate size. Figure 11 shows the shear strength as a function of the aggregate size. An outline of the figure was given with a fitting line of a logarithmic function. The shear strength increased with the

Fig. 10 SEM images of the copper stages after the measurement of shear strength. The particles used for the measurements were prepared at the reaction temperatures of **a** 5, **b** 20, **c** 30, **d** 50, and **e** 80 °C
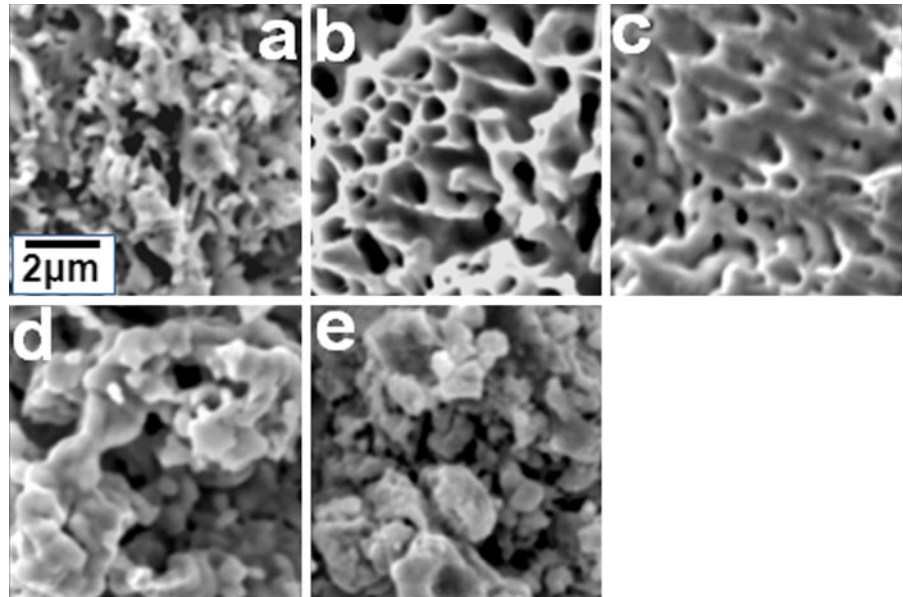
increase in the aggregate size. The large aggregates were produced at 20 °C, which meant that each CuO nanoparticle was located close to other CuO nanoparticles, i.e., the powder of CuO particles was dense. Probably, for 20 °C, the metallic Cu particles that were produced from the CuO nanoparticles were fused more easily because of the denseness. Consequently, the fusion resulted in the strong bonding.

Conclusions

Metallic bonding with the use of CuO nanoparticles was demonstrated. CuO nanoparticles were prepared by reacting $Cu(NO_3)_2$ with NaOH in aqueous solution. A reaction at 20 °C resulted in production of large leaf-like aggregates composed of CuO nanoparticles with an average size of ca., 10 nm. The aggregate size decreased with the increase in reaction temperature. Bonding examination was performed sandwiching the CuO nanoparticles between copper discs and pressurizing them at 1.2 MPa for 5 min in H_2 gas at 400 °C. A shear strength required for separating the discs were 25.4 MPa for the CuO nanoparticles prepared at 20 °C. The shear strength tended to decrease with the increase in reaction temperature. Possibly, the formation of aggregates
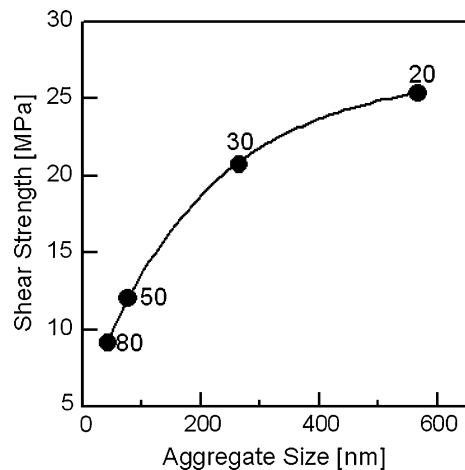

Fig. 11 Plot of the shear strength versus the aggregate size. Numbers stand for the reaction temperatures (°C)

made the powder of CuO particles dense, which accelerated the fusion of metallic copper particles produced from the CuO particles and consequently provided efficient metallic bonding. The present work demonstrated feasibility of metallic bonding with the use of metal oxide.

References

Akada Y, Tatsumi H, Yamaguchi T, Hirose A, Morita T, Ide E (2008) Interfacial bonding mechanism using silver metallo-organic nanoparticles to bulk metals and observation of sintering behavior. Mater Trans 49:1537–1545

Buffat P, Borel JP (1976) Size effect on the melting temperature of gold particles. Phys Rev A 13:2287–2298

Ide E, Angata S, Hirose A, Kobayashi KF (2005) Metal-metal bonding process using Ag metallo-organic nanoparticles. Acta Mater 53:2385–2393

Kanninen P, Johans C, Merta J, Kontturi K (2008) Influence of ligand structure on the stability and oxidation of copper nanoparticles. J Colloid Interface Sci 318:88–95

Lee SH, Her YS, Matijević E (1997) Preparation and growth mechanism of uniform colloidal copper oxide by the controlled double-jet precipitation. J Colloid Interface Sci 186:193–202

Liu Q, Liu H, Liang Y, Xu Z, Yin G (2006) Large-scale synthesis of single-crystalline CuO nanoplatelets by a hydrothermal process. Mater Res Bull 41:697–702

Matsuoka S, Imai H (2009) Direct welding of different metals used ultrasonic vibration. J Mater Process Technol 209:954–960

Moon K, Dong H, Maric R, Pothukuchi S, Hunt A, Li Y, Wong CP (2005) Thermal behavior of silver nanoparticles for low-temperature interconnect applications. J Electron Mater 34:168–175

Morita T, Ide E, Yasuda Y, Hirose A, Kobayashi K (2008a) Study of bonding technology using silver nanoparticles. Jpn J Appl Phys 47:6615–6622

Morita T, Yasuda Y, Ide E, Akada Y, Hirose A (2008b) Bonding technique using micro-scaled silver-oxide particles for in situ formation of silver nanoparticles. Mater Trans 49:2875–2880

Morita T, Yasuda Y, Ide E, Akada Y, Hirose A (2009) Direct bonding to aluminum with silver-oxide microparticles. Mater Trans 50:226–228

Murray AJ, Jaroenapibal P, Koene B, Evoy S (2006) Sintering of silver nanoparticles for the formation of high temperature interconnect joints. Mater Res Soc Symp Proc 942E:W08–W29

Park BK, Kim D, Jeong S, Moon J, Kim JS (2007) Direct writing of copper conductive patterns by ink-jet printing. Thin Solid Films 515:7706–7711

Takagi M (1954) Electron-diffraction study of liquid-solid transition of thin metal films. J Phys Soc Jpn 9:359–363

Weisman C (ed) (1976) Welding handbook, vol 1, 7th edn. American Welding Society, Miami, pp 18–19

Yasuda Y, Ide E, Morita T (2009) Low-temperature bonding using silver nanoparticles stabilized by short-chain alkylamines. Jpn J Appl Phys 48:125004

Zheng L, Liu X (2007) Solution-phase synthesis of CuO hierarchical nanosheets at near-neutral pH and near-room temperature. Mater Lett 61:2222–2226